Proposed Photosynthesis Method for Producing Hydrogen from Dissociated Water Molecules Using Incident Near-Infrared Light

Xingxing Li,[1] Zhenyu Li,[1,2] and Jinlong Yang[1,2,*]
[1]Hefei National Laboratory of Physical Science at the Microscale, University of Science and Technology of China, Hefei, Anhui 230026, China
[2]Synergetic Innovation Center of Quantum Information and Quantum Physics, University of Science and Technology of China, Hefei, Anhui 230026, China
(Received 23 June 2013; published 8 January 2014)

Highly efficient solar energy utilization is very desirable in photocatalytic water splitting. However, until now, the infrared part of the solar spectrum, which constitutes almost half of the solar energy, has not been used, resulting in significant loss in the efficiency of solar energy utilization. Here, we propose a new mechanism for water splitting in which near-infrared light can be used to produce hydrogen. This ability is a result of the unique electronic structure of the photocatalyst, in which the valence band and conduction band are distributed on two opposite surfaces with a large electrostatic potential difference produced by the intrinsic dipole of the photocatalyst. This surface potential difference, acting as an auxiliary booster for photoexcited electrons, can effectively reduce the photocatalyst's band gap required for water splitting in the infrared region. Our electronic structure and optical property calculations on a surface-functionalized hexagonal boron-nitride bilayer confirm the existence of such photocatalysts and verify the reaction mechanism.

DOI: 10.1103/PhysRevLett.112.018301 PACS numbers: 82.50.Nd, 73.22.-f, 81.05.Zx, 82.47.-a

As an ultimate solution for today's more and more serious energy and environmental problems, solar energy is abundant and clean, and it can be converted into chemical fuel, biomass, or electricity, or directly stored as thermal energy. An important branch of solar-to-chemical energy conversion, hydrogen production from photocatalytic water splitting, viewed as an artificial photosynthesis, has been eagerly pursued since its first proposal in 1972 [1].

The key issue in photocatalytic water splitting is to develop photocatalysts with high solar energy conversion efficiency. Solar energy is distributed in ultraviolet, visible, and infrared light with a proportion of about 7%:50%:43%. However, traditional photocatalysts based on metal oxides [2–5], sulfides [6,7], nitrides [8,9], oxynitrides [10], oxysulfides [11], etc., are mostly active only under ultraviolet irradiation, while other photocatalysts which absorb visible light are not stable during the reaction process, such as the photocorrosion for metal sulfide photocatalysts, or the quantum yield under visible light is relatively low (usually under 10%), leading to a very inefficient usage of sunlight. To solve these problems, many methods have been pursued: first, reduce the band gap of photocatalyst into the visible light region through band-gap engineering, for example, by cation or anion (co-)doping [12,13]; second, avoid photocorrosion by employing sacrificial reagents, e.g., electron donors or hole scavengers; third, design a new reaction mechanism, e.g., the **Z**-scheme systems (two-photon process) [14,15]; last, explore novel kinds of photocatalysts, e.g., metal-free photocatalysts [16–19].

Compared to the abundance of works done in the visible light area, the infrared part of the solar spectrum has been overlooked. Since infrared light encompasses almost half the solar energy, if using infrared light for hydrogen production were realized, then the efficiency of solar energy utilization would be largely improved. However, further reducing the photocatalyst's band gap from the visible light region into the infrared region is impossible with the standard reaction mechanism of water splitting: the band gap of the photocatalyst must be larger than 1.23 eV as the difference of reduction and oxidation potentials of water splitting [20]. To break through this restriction, a new mechanism is needed.

With the design of a new photocatalyst, we propose in this Letter a novel reaction mechanism for water splitting in which utilizing infrared light for hydrogen production can be readily achieved. Such infrared-light-driven water splitting opens a new future for solar energy conversion.

A schematic map of our new photocatalytic model is shown in Fig. 1. We first consider a system composed of two identical photocatalysts in nanoscale under the normal model in Fig. 1(a): The energy levels of both the reduction potential ($V_{H^+\text{-}H_2} = 4.44$ eV) [16] for H^+ to H_2 and the oxidation potential ($V_{O_2\text{-}H_2O} = 5.67$ eV) of H_2O to O_2 are located inside the band gap. When we apply an external electric field in the space between the two photocatalysts [Fig. 1(b)], all the energy levels bend along the direction of the electric field. Interestingly, supposing the two photocatalysts are merged into one with a self-induced internal electric field, the band bending leads to the formation of nanoheterojunction with the charge distribution of the whole system's valence band (VB) on one surface and its conduction band (CB) on the other. Without losing generality, we call these two surfaces the $(00\bar{1})$ and (001) surfaces. In practice, this internal electric field can be

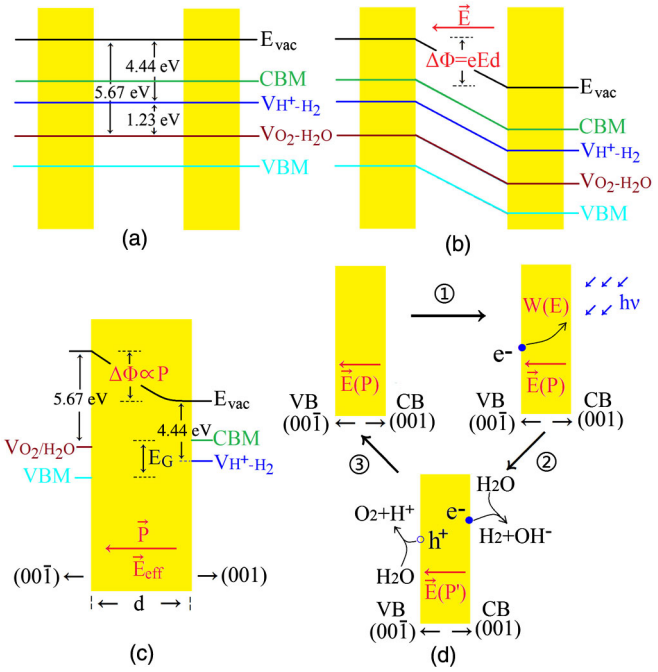

FIG. 1 (color online). A schematic plot of energy levels for a two-photocatalyst system: (a) undisturbed, and (b) when an external electric field is applied between them; (c) a one-photocatalyst system with an internal effective electric field E_{eff} produced by its intrinsic dipole **P**; (d) the reaction process of photocatalytic water splitting in our new model. E_{vac} stands for vacuum level, and CBM and VBM are the conduction-band minimum and valence-band maximum, respectively.

self-introduced by the junction's intrinsic dipole **P** according to the following equation

$$E_{\text{eff}} = \frac{P}{\varepsilon S d}, \tag{1}$$

in which ϵ is the dielectric constant, S is the surface area, and d is the thickness of the junction. Obviously, to produce a notable effective electric field, d should be small enough, e.g., a few nanometers. Because of the band bending induced by the internal electric field, from Fig. 1(c), one can see that the difference between the oxidation potential on the (00$\bar{1}$) surface and the reduction potential on the (001) surface is now reduced from 1.23 eV to 1.23 eV $-$ $\Delta\Phi$, where $\Delta\Phi$ is the electrostatic potential difference between two surfaces:

$$\Delta\Phi = \frac{ep}{\varepsilon S}. \tag{2}$$

The conditions of photocatalytic water splitting for this system are as follows: on the (00$\bar{1}$) surface, the oxidation potential should be located above the valence band maximum (VBM), while, on the (001) surface, the reduction potential should be located below the conduction band minimum (CBM). Therefore, the restriction on the photocatalyst's band gap is

$$E_G > 1.23 - \Delta\Phi, \qquad E_G > 0. \tag{3}$$

Increasing by tuning the intrinsic dipole, the band gap of the photocatalyst can then be reduced to the infrared region. For large values of $\Delta\Phi$, i.e., $\Delta\Phi > 1.23$ eV, there is no restriction on the band gap.

Upon absorbing an infrared photon, an electron is excited from VB to CB, producing a hole on (00$\bar{1}$) and an electron on (001). This process is similar to the strong charge-transfer transitions widely observed in donor-accepter molecular systems [21,22]. In this process, the internal electric field does positive work on the electron

$$W = eEd = \Delta\Phi, \tag{4}$$

since now the required photon energy is less than that in systems without an intrinsic dipole (see Fig. S1 in Supplemental Material [23]). After the electron is excited to reside on the (001) surface, the internal electric field prevents it from going back to the (00$\bar{1}$) surface, resulting in a perfect spatial separation of the photogenerated electron-hole pair. Then, on the (001) surface, the water molecule or proton grasps the excited electron, being reduced to H_2, while on the (00$\bar{1}$) surface, the hole is transferred to the water molecule, oxidizing it to O_2. The overall photocatalytic reaction process is illustrated in Fig. 1(d).

Our proposed photocatalytic model possesses at least two distinct advantages: one is to relieve the restriction on the photocatalyst's band gap; the other is the perfect charge separation for photogenerated electron-hole pairs. The next important step is to find a real material with such properties. Based on first-principles density functional theory calculations, we show that surface-functionalized boron-nitride (BN) bilayer (F-BNBN-H) is a good candidate. All our calculations are carried out within the Perdew-Burke-Ernzerhof generalized gradient approximation (GGA) [24] implemented in the Vienna *ab initio* simulation package (VASP) [25]. The projector augmented wave potential [26] and the plane-wave cutoff energy of 400 eV are used. The first Brillouin zone is sampled with a Monkhorst-Pack grid of $15 \times 15 \times 1$. Both the lattice constant and the positions of all atoms are relaxed until the force is less than 0.01 eV/Å. The criterion for the total energy is set as 1×10^{-5} eV. A vacuum space of 30 Å along the z direction is used to eliminate the interaction of neighboring junctions. Since the GGA approach usually underestimates the band gap of a semiconductor, the screened hybrid Heyd-Scuseria-Ernzerhof 2006 (HSE06) functional [27,28] is then adopted to get accurate electronic structures and optical properties. For optical properties, we first calculate the imaginary part of the frequency-dependent dielectric function [29]; then the optical absorption coefficients can be evaluated.

The optimized structure is shown in Fig. 2(a). In this structure, the BN bilayer possesses a low-energy *AB* stacking structure. H and F atoms sit on N and B atoms, respectively, which generates a large intrinsic dipole (1.58 D per

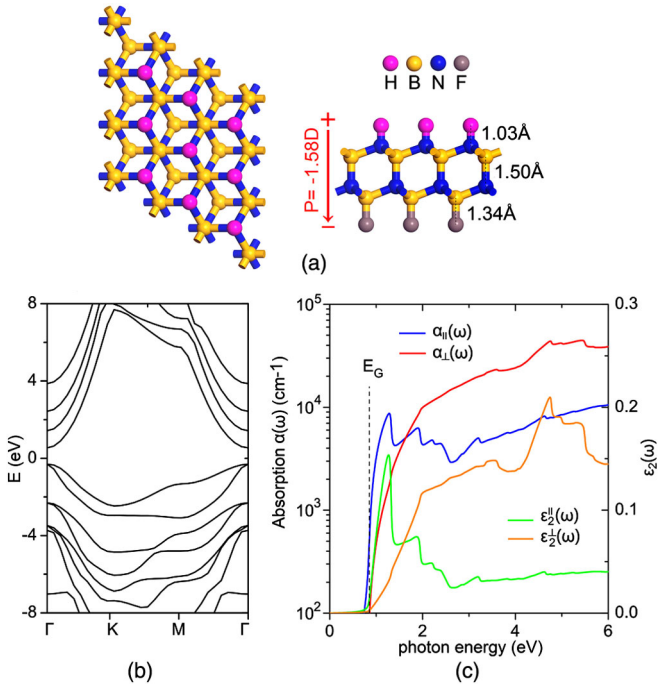

FIG. 2 (color online). (a) The optimized structure of F-BNBN-H, top view (left) and side view (right). (b) The electronic band structure of F-BNBN-H with HSE06 functional. (c) The frequency-dependent imaginary dielectric function $\varepsilon_2(\omega)$and optical absorption coefficients $\alpha(\omega)$ with the polarization vector parallel and perpendicular to the z axis.

unit cell). The next question is whether the structure is stable. We first calculate the formation energy with respect to the hexagonal BN sheet, free H_2 and F_2 molecules, and find it is -0.405 eV per atom. That value is negatively large, implying that the formation of F-BNBN-H is exothermic and thus energetically favored. The combination of two functionalized single layers, F-BN and BN-H, turns out to be barrierless. (See Fig. S2 in Supplemental Material [23].) At the same time, first-principles MD simulations of freestanding F-BNBN-H and its water solution lasting for 2 ps do not show any significant structure distortion (Fig. S3 in Supplemental Material [23]), which demonstrates the good stability of F-BNBN-H.

The electronic band structure calculated with GGA has a tiny gap (Fig. S4 in Supplemental Material [23]), and a more accurate gap obtained by HSE06 is 0.85 eV [Fig. 2(b)], corresponding to an absorption in the near-infrared region of the solar spectrum. To see whether IR absorption can take place in practice, the frequency-dependent imaginary dielectric function and absorption coefficients are computed [Fig. 2(c)]. There is a relatively strong absorption near 1.25 eV with intensity up to 10^4 cm^{-1}, mainly contributed from transitions of VB to CB around the $\mathbf{\Gamma}$ k point. One can see that the optical gap matches well with the electronic band gap.

We next examine the spatial distribution of VB and CB. We find that the charge density of VB is mainly located around F atoms and N atoms of the lower-lying BN layer, while CB consists of nearly-free-electron (NFE) states residing upside of the (001) surface and a minority density at N atoms of the upper-lying BN layer [Figs. 3(a) and 3(b)]. In summary, VB is distributed on the (00$\bar{1}$) surface and CB on the (001) surface, which is consistent with our photocatalytic model. The good charge separation of VB and CB can effectively reduce the probability of recombination of photogenerated electrons and holes and ensure the photocatalytic activity. Another important integrant of our model is the dipole-induced internal electric field or surface potential difference. For F-BNBN-H, the potential difference for the (00$\bar{1}$) and (001) surfaces is found to be 10.0 eV [Fig. 3(c)], which is large enough to cause notable band bending across the junction.

Next by employing the HSE06 functional, accurate energy locations of valence band maximum and conduction band minimum with respect to the redox potentials of water splitting are determined, as shown in Fig. 4 together with the surface projected density of states. On the (00$\bar{1}$) surface, the oxidation potential $V_{O_2\text{-}H_2O}$ is higher than VBM by about 5.76 eV, implying that photogenerated holes can be readily transferred from valence band to H_2O, oxidizing it to O_2:

$$2H_2O + 4h^+ \rightarrow O_2 + 4H^+. \quad (5)$$

Meanwhile on the (001) surface, as the reduction potential $V_{H^+\text{-}H_2}$ lies below CBM by about 3.86 eV, the photoexcited

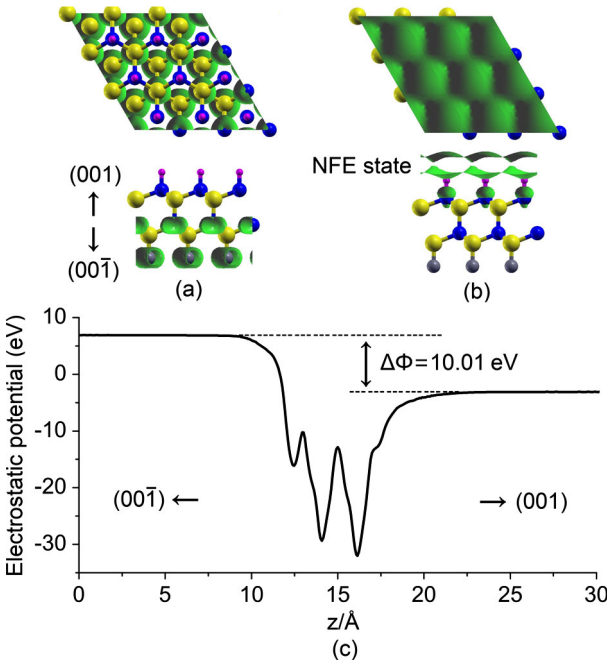

FIG. 3 (color online). The charge distribution of the (a) valence band and (b) conduction band for F-BNBN-H with an isovalue of 0.09 e/Å^3. (c) The calculated electrostatic potential difference of the (00$\bar{1}$) and (001) surfaces.

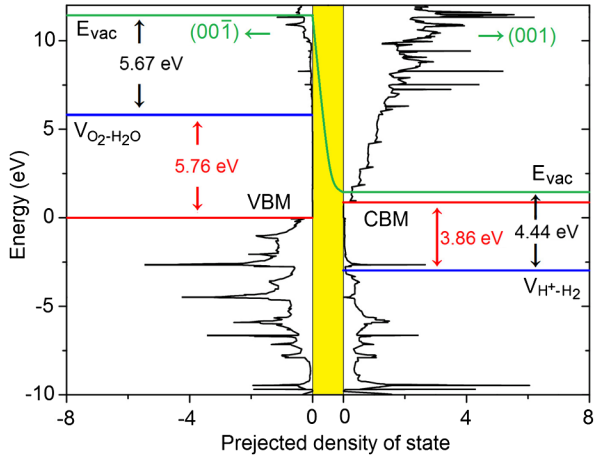

FIG. 4 (color online). Energy diagram for F-BNBN-H. The surface-projected density of states is plotted with black lines. The energy locations of vacuum level (E_{vac}), redox potentials of water ($V_{O_2\text{-}H_2O}$, $V_{H^+\text{-}H_2}$), VBM, and CBM are denoted as labeled straight lines.

electron in the conduction band promptly flows down to H_2O or H^+, producing H_2:

$$4H_2O + 4e^- \rightarrow 2H_2 + 4OH^-. \quad (6)$$

To finish the whole reaction, the protons H^+ produced on the (00$\bar{1}$) surface must be transferred to the (001) surface. If we are only interested in hydrogen generation, sacrificial reagents reacting with hydroxyl ions OH^- can be used to promote the production of hydrogen. Also notice that the large potential energy differences between redox potentials and VBM-CBM provide a large driving force for the reaction, and overpotential caused by kinetic barriers is expected to be easily overcome.

Therefore, F-BNBN-H acts as a promising near-infrared-light-driven photocatalyst for water splitting. Furthermore, from the surface-projected density of states, one can see that the conduction band states up to 5.0 eV are all distributed mainly on the (001) surface, allowing a broad range of optical absorption (from near-infrared to ultraviolet) while maintaining a very good spatial separation for photogenerated electron-hole pairs.

In our model, the photocatalyst's intrinsic dipole plays an important role in determining the internal electric field and thus the surface potential difference. In a real environment, there are water molecules around. To check their effects on the intrinsic dipole layer, we place H_2O molecules on both the (00$\bar{1}$) and (001) surfaces of F-BNBN-H with an adsorption concentration of 1/9 ML (Fig. S5 in Supplemental Material [23]). The highest occupied molecular orbitals of H_2O molecules are shifted apart from each other by a large energy distance of about 5.7 eV, with the one on the (001) surface lower in energy (Fig. S6 in Supplemental Material [23]), which directly demonstrates the existence of a large potential difference between (00$\bar{1}$) and (001) surfaces. A higher adsorption concentration (1 ML H_2O) is also tested, and the energy shift of highest occupied molecular orbitals is almost the same (see Figs. S7 and S8 in Supplemental Material [23]). This result confirms the robustness of surface potential difference when the photocatalyst is immersed in water.

Another important issue about our photocatalytic model is the system's sustainability. In the model, the absorbed photon energy together with the positive work produced by the internal effective electric field of the photocatalyst is used to drive the endothermic water-splitting reaction, and, in this way, the energy of the whole system is conserved. However, the generated protons and hydroxyl ions during the reaction process [Fig. 1(d)] will be bound on the photocatalyst's surfaces, causing a gradual decrease of internal electric field, and finally the reactions stop. To resume the reaction, the protons and hydroxyl ions should be removed from the surfaces, which can be done by several means. A natural choice can be pulsed electric field, or a sacrificial reagent can be used. It is also possible to use mechanical means such as supersonic processing to remove surface blockers. Another solution is to make the photocatalyst porous [30,31]; the protons can easily go through the pores to combine with the hydroxyl ions. It is also possible to construct a hybrid photocatalyst with other materials [32–34]. For example, we can load TiO_2 and Pt nanoparticles on (00$\bar{1}$) and (001) surfaces, respectively, to accept the photogenerated holes and electrons, and then the water splitting reaction will continue at the site of TiO_2 and Pt nanoparticles, with produced protons and hydroxyl ions far away from the surfaces.

In our model, the broad absorption from near-infrared light to ultraviolet light along with the perfect spatial separation of photogenerated electron-hole pairs ensures a very good conversion efficiency of sunlight, which is the main merit of our proposal and it has not been realized before. Then, the overall efficiency is determined as the ratio of other energy required to regenerate the dipole in the whole energy input. Since activity regeneration mainly involves moving physically adsorbed ions, the additional energy required is expected to be much smaller than the energy required to break the chemical bonds in water. Therefore, the overall efficiency should also be relatively high.

Based on the example of F-BNBN-H, we have a great flexibility to design photocatalysts using hybrid BN-C layers with various magnitudes of intrinsic dipole layer and surface potential difference. We have tested three other systems, and we find that they are all potential photocatalysts with their band gaps ranging from the visible light region to the near-infrared light region. (For details, see Figs. S9–S12 in Supplemental Material [23].) Furthermore, due to the existence of the strong ionic bond, the exposed surfaces of transition metal oxides, such as ZnO nanorods [35], are expected to also have large intrinsic

dipoles. Guided by a careful design, these materials may also be explored for near-infrared-driven photocatalysts. At the same time, our photocatalytic model described here is not restricted to water splitting; it can be extended to all other photocatalytic systems, for example, the photodegradation of contamination. Thus, by employing specifically designed photocatalysts based on our model, large-scale utilization of the infrared part of solar energy in photocatalysis can be realized.

In conclusion, we have proposed a new photocatalytic model in which near-infrared light can be utilized for hydrogen production from photocatalytic water splitting. The new model is then verified in surface-functionalized hexagonal boron-nitride bilayers by first-principles electronic and optical calculations. Application of our model to other photocatalytic processes is possible, presenting a promising future for near-infrared-light-driven photocatalysis.

This work is partially supported by the National Key Basic Research Program (Contract No. 2011CB921404), by NSFC (Contracts No. 21121003, 91021004, 20933006, 21233007, 21222304), by CAS (Contract No. XDB01020300), and by USTCSCC, SCCAS, Tianjin, and Shanghai Supercomputer Centers.

*jlyang@ustc.edu.cn

[1] A. Fujishima and K. Honda, Nature (London) **238**, 37 (1972).
[2] K. Yamaguti and S. Sato, J. Chem. Soc., Faraday Trans. **81**, 1237 (1985).
[3] K. Domen, S. Naito, M. Soma, T. Onishi, and K. Tamaru, J. Chem. Soc. Chem. Commun. **1980**, 543 (1980).
[4] J. Sato, H. Kobayashi, N. Saito, H. Nishiyama, and Y. Inoue, J. Photochem. Photobiol., A, **158**, 139 (2003).
[5] T. Yanagida, Y. Sakata, and H. Imamura, Chem. Lett. **33**, 726 (2004).
[6] M. Matsumura, Y. Saho, and H. Tsubomura, J. Phys. Chem. **87**, 3807 (1983).
[7] J. F. Reber and K. Meier, J. Phys. Chem. **88**, 5903 (1984).
[8] J. Sato, N. Saito, Y. Yamada, K. Maeda, T. Takata, J. N. Kondo, M. Hara, H. Kobayashi, K. Domen, and Y. Inoue, J. Am. Chem. Soc. **127**, 4150 (2005).
[9] K. Maeda, K. Teramura, N. Saito, Y. Inoue, and K. Domen, Bull. Chem. Soc. Jpn. **80**, 1004 (2007).
[10] G. Hitoki, T. Takata, J. N. Kondo, M. Hara, H. Kobayashi, and K. Domen, Chem. Commun. (Cambridge) **02**, 1698 (2002).
[11] A. Ishikawa, T. Takata, J. N. Kondo, M. Hara, H. Kobayashi, and K. Domen, J. Am. Chem. Soc. **124**, 13547 (2002).
[12] Z. Zou, J. Ye, K. Sayama1, and H. Arakawa, Nature (London) **414**, 625 (2001).
[13] R. Konta, T. Ishii, H. Kato, and A. Kudo, J. Phys. Chem. B **108**, 8992 (2004).
[14] K. Sayama, K. Mukasa, R. Abe, Y. Abe, and H. Arakawa, J. Photochem. Photobiol., A **148**, 71 (2002).
[15] H. Kato, M. Hori, R. Konta, Y. Shimodaira, and A. Kudo, Chem. Lett. **33**, 1348 (2004).
[16] X. Wang, K. Maeda, A. Thomas, K. Takanabe, G. Xin, J. M. Carlsson, K. Domen, and M. Antonietti, Nat. Mater. **8**, 76 (2009).
[17] G. Liu, P. Niu, L. Yin, and H. Cheng, J. Am. Chem. Soc. **134**, 9070 (2012).
[18] F. Wang, W. K. H. Ng, J. C. Yu, H. Zhu, C. Li, L. Zhang, Z. Liu, and Q. Li, Appl. Catal., B **111**, 409 (2012).
[19] J. Liu, S. Wen, Y. Hou, F. Zuo, G. J. O. Beran, and P. Feng, Angew. Chem., Int. Ed. Engl. **52**, 1 (2013).
[20] A. Kudo and Y. Miseki, Chem. Soc. Rev. **38**, 253 (2009).
[21] F. Riobé, P. Grosshans, H. Sidorenkova, M. Geoffroy, and N. Avarvari, Chem. Eur. J. **15**, 380 (2009).
[22] F. Pop, F. Riobé, S. Seifert, T. Cauchy, J. Ding, N. Dupont, A. Hauser, M. Koch, and N. Avarvari, Inorg. Chem. **52**, 5023 (2013).
[23] See Supplemental Material at http://link.aps.org/supplemental/10.1103/PhysRevLett.112.018301 for details about the physical meaning of work done by the dipole field; the formation reaction pathway and MD simulation for F-BNBN-H; the comparison between PBE and HSE06 functionals; the adsorption calculations of H_2O on F-BNBN-H; and predictions of three other potential photocatalysts.
[24] J. P. Perdew, K. Burke, and M. Ernzerhof, Phys. Rev. Lett. **77**, 3865 (1996).
[25] G. Kresse and J. Furthmüller, Phys. Rev. B **54**, 11169 (1996).
[26] P. E. Blöchl, Phys. Rev. B **50**, 17953 (1994).
[27] J. Heyd, G. E. Scuseria, and M. Ernzerhof, J. Chem. Phys. **118**, 8207 (2003).
[28] J. Heyd, G. E. Scuseria, and M. Ernzerhof, J. Chem. Phys. **124**, 219906 (2006).
[29] M. Gajdoš, K. Hummer, G. Kresse, J. Furthmüller, and F. Bechstedt, Phys. Rev. B **73**, 045112 (2006).
[30] P. Hartmann, D. K. Lee, B. M. Smarsly, and J. Janek, ACS Nano **4**, 3147 (2010).
[31] C. Liang, Z. Li, and S. Dai, Angew. Chem., Int. Ed. Engl. **47**, 3696 (2008).
[32] R. Saito, Y. Miseki, and K. Sayama, Chem. Commun. (Cambridge) **48**, 3833 (2012).
[33] A. K. Agegnehu, C. J. Pan, J. Rick, J. F. Lee, W. N. Su, and B. J. Hwang, J. Mater. Chem. **22**, 13849 (2012).
[34] Y. Liang, Y. Li, H. Wang, and H. Dai, J. Am. Chem. Soc. **135**, 2013 (2013).
[35] S. Dag, S. Wang, and L. W. Wang, Nano Lett. **11**, 2348 (2011).